LETTERS
PUBLISHED ONLINE: 11 OCTOBER 2009 | DOI: 10.1038/NGEO656
nature geoscience

Deep slab hydration induced by bending-related variations in tectonic pressure

Manuele Faccenda[1]*, Taras V. Gerya[1] and Luigi Burlini[2]

Bending of oceanic plates at subduction zones results in extension and widespread normal faulting[1] in the upper, brittle part of the slab[2,3]. Detailed seismic surveys at trenches reveal that this part of the oceanic plate could be pervasively hydrated for several kilometres below the crust–mantle boundary[4–7]. Similarly, heat-flow surveys indicate active fluid circulation within the slab[8]. Yet, the mechanisms that enable fluids to percolate to such depths in spite of their natural buoyancy remain unclear. Here we use two-dimensional numerical experiments to show that stress changes induced by the bending oceanic plate produce subhydrostatic or even negative pressure gradients along normal faults, favouring downward pumping of fluids. The fluids then react with the crust and mantle surrounding the faults and are stored in the form of hydrous minerals. We suggest that this process is the dominant mechanism of deep slab hydration, although it may be locally aided by the enhancement in porosity due to prefailure dilatancy[9], pre-existing cracks[10] and migrating fluid-filled cracks[11]. Our results have implications for the transport of water into the deeper parts of the mantle[12], and for further clarifying the seismic anisotropy of slabs[13].

Hydration of the oceanic crust occurs mainly at mid-ocean ridges in response to the high porosity and permeability produced by lava drainbacks, fissuring, inter-unit voids, normal faulting and volume decrease due to thermal contraction[2,14]. Hydrothermal fluid circulation can occur within plates with an average age up to 65 million year (Myr), which may significantly contribute to further oceanic plate hydration[14]. For instance, oceanic plates formed at fast-spreading (for example, Pacific-type) mid-ocean ridges show brittle fracturing and are hydrothermally altered in the upper 2–3 km of the crust[2]. In deep and old oceanic basins, mean upper crustal porosities of 12% have been reported, leading to the concept of a global-scale fluid reservoir residing within the uppermost, basaltic oceanic crust where nearly 2% of the total volume of global sea water is contained[14]. The process of oceanic crust hydration has been systematically studied and is thought to be well understood. However, evidence of oceanic plate hydration at the outer rise of trenches, down to mantle depths[4–8], poses the serious problem of how sea water can penetrate deeply in the slab. Seismic pumping (that is, preseismic opening of dilatational jogs along faults, see ref. 9 for a review) and thermal cracking (see, for example, ref. 10) are commonly invoked as possible mechanisms to drive fluids into bending-related normal faults or old oceanic plates, respectively. Another mechanism to move fluids along shear zones is by Vug waves: a coupled deformation/fluid-migration mechanism in which a rock deforms by the movement of a fluid-filled crack dislocation across a plane of shear, with the migration of the crack and fluid driven by the release of elastic shear strain energy[11]. However, it is unclear whether such crack-opening mechanisms are sufficient to explain entirely seawater percolation several tens of kilometres down into the slab. In contrast, variations of the tectonic pressure, affecting a region as long as the whole shear zone (see, for example, ref. 15), seem to provide a more appropriate and efficient mechanism for pumping fluid downward in these extensional settings.

Dynamic pressure is defined as the average of the normal components of the stress tensor. In a system at rest, dynamic pressure is equal to the lithostatic pressure and all the normal stress components have the same magnitude. When deviatoric stresses are applied to the system, the positive (or negative) difference between the solid (dynamic) pressure and the lithostatic pressure is called tectonic overpressure (or underpressure; see ref. 15 for a complete review and discussion). Distributed tectonic overpressure is characteristic of compressional regimes and viscous (ductile) shear zones. In contrast, tectonic underpressure is typical of extensional regimes and tends to focus along brittle Mohr–Coulomb faults, creating conditions for fluid pumping inside these faults. More importantly, it is the gradient in tectonic pressure, rather than its absolute magnitude, that is fundamental for driving fluid flow from high-pressure regions into low-pressure regions[15]. For instance, it has been found recently that, in a deforming ductile material, dynamic pressure gradients have a crucial role in driving fluid flow, leading to the spontaneous segregation of melt-rich bands[16].

To explore the effects of tectonic pressure on bending-related hydration of the slab, we carried out two-dimensional numerical experiments in which an oceanic plate bends spontaneously under the control of realistic visco-elasto-plastic rheologies (see Methods for further details of the numerical model). The upper, 2-km-thick, basaltic layer of the oceanic crust is treated as a highly porous and fluid-saturated reservoir (see, for example, ref. 14; see the above discussion), where fluid markers are placed. The lower, 6-km-thick, gabbroic crust is dry. Assuming that with increasing depth and decreasing porosity below the oceanic floor the dynamic pressure in the solid phases and the fluid pressure will approach each other, we computed the fluid flow below 2 km depth (that is, below the fluid-saturated reservoir) according to the dynamic pressure gradients estimated from our thermomechanical numerical model (see the Supplementary Methods section for explanations regarding the fluid-flow-model assumptions):

$$v_z = -\frac{k}{\phi\mu}\left(\frac{\partial P}{\partial z} - g\rho_{\text{fluid}}\right)$$

$$v_x = -\frac{k}{\phi\mu}\frac{\partial P}{\partial x}$$

where v_x and v_z are the horizontal and vertical components of the pore-fluid velocity vector, z is the depth, k is the effective

[1]Geophysical Fluid Dynamics, Institute of Geophysics, ETH Zürich, Sonneggstr. 5, 8092 Zürich, Switzerland, [2]Institute of Geology, ETH Zürich, Sonneggstr. 5, 8092 Zürich, Switzerland. *e-mail: manuele.faccenda@gmail.com.

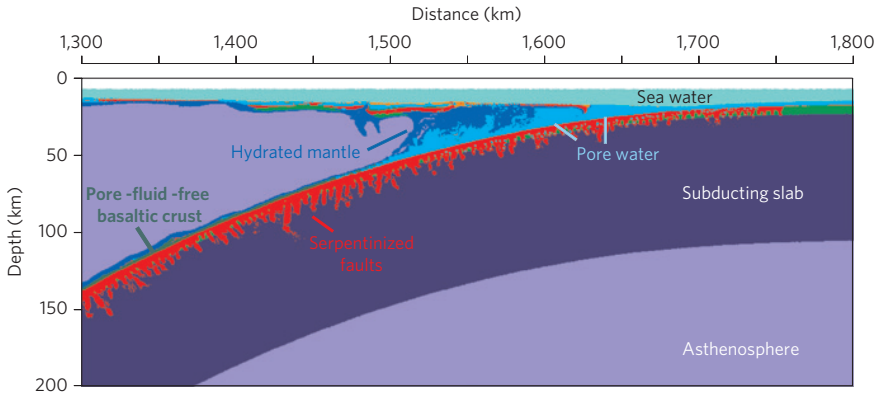

Figure 1 | Thermomechanical two-dimensional model of a spontaneously bending oceanic plate. Compositional map. Serpentinized faults are trenchward dipping but sets of antithetic and seaward-dipping faults are occasionally visible. Light green is dry, gabbroic oceanic crust; dark green is pore-fluid-free, basaltic oceanic crust; orange is sediments. Light blue is pore water present initially in the basaltic layer that is either pumped downward producing serpentinization (red) or, as the slab subducts, is expelled upward into the overlying mantle wedge (blue) and accretionary prism (see also Fig. 2a). The age of the slab at the trench is approximately 50 Myr.

permeability (5×10^{-18} m^2), ϕ is the effective porosity (0.01), μ is the fluid viscosity (10^{-4} Pa s), P is dynamic pressure (Pa), ρ_{fluid} is the fluid density (1,000 kg m^{-3}) and $g = 9.81$ m s^{-2} is the gravitational acceleration directed downward. The effective hydraulic parameters used in the model correspond to a broad range of crystalline rocks with poor hydraulic properties (either unfractured or postfailure rocks[17,18]) and correspond to a time-integrated hydraulic behaviour of shear zones among the various phases of porosity enhancement and reduction. To better distinguish the effects of tectonic pressure from those of cracking, our models do not take into account volume dilatancy produced by crack opening (that is, the dilatation angle is assumed to be zero).

As shown in Figs 1, 2f and Supplementary Fig. S2, hydration and the associated serpentinization of the slab is pervasive down to a few tens of kilometres below the Moho. Brittle normal faults propagate from the top to the central part of the slab (Fig. 2b), favouring hydration by fluids percolating downward from the upper, fluid-saturated crustal layer (Fig. 2a). Fault activation due to the bending of the plate starts at shallow depths, offshore of the trench, and progressively deepens as the faults move through the slab bending zone. Fault propagation is assisted by gradual serpentinization, which promotes rheological weakening of the shear zone, more localized deformation and a larger tectonic underpressure (see Supplementary Fig. S2 for the time evolution of a serpentinizing fault). The downward water pumping is driven by the inverted (that is, subhydrostatic $\partial P/\partial z < g\rho_{\mathrm{fluid}}$, or even negative $\partial P/\partial z < 0$) vertical pressure gradients focused along brittle normal faults (Fig. 2b–d, Supplementary Fig. S2), which favour localized patterns of fluid flow and associated serpentinization (Figs 1 and 2a). The numerous inverted pressure gradients (Fig. 2e) typically form on the upper boundary of the fault planes as a consequence of the dense inter-layering areas of low deformation (Fig. 2b, light blue/greenish) and weak tectonic underpressure (Fig. 2c, d, Supplementary Fig. S2, light blue/greenish). Such occurrences are overlying either active, new (for example, at the outer rise, Fig. 2b, red), or deactivating, old (below the overriding plate), faults that are characterized by ongoing, or completed, rheological weakening due to brittle/plastic deformation and serpentinization (see Methods and Supplementary Table S1) and by strong tectonic underpressure (Fig. 2c–e, Supplementary Fig. S2, deep blue). Conditions for downward fluid flow are met in proximity to the trench and below the fluid-saturated overriding plate, where the slab curvature and inverted pressure gradients are high and the downward fluid pumping is maximal (Fig. 2c). Trenchward- (synthetic) and seaward- (antithetic) dipping faults are favourable sites for plate hydration at the outer rise. In contrast, slab hydration below the overriding plate occurs mainly along antithetic, seaward-dipping faults.

Slab hydration is favoured by a thick, fluid-saturated reservoir present in the crust before bending (Supplementary Fig. S3) and by small amounts of rheological weakening of the brittle and hydrating faults (Supplementary Figs S5 and S6). In contrast, a very low effective permeability of the slab prevents fluids from percolating pervasively to large depths (Supplementary Fig. S4; see Supplementary Discussion section).

The results of the numerical experiment are consistent with low-seismic-velocity areas present in the upper part of the Cocos and Nazca slabs, which were interpreted as the result of serpentinization[4–6]. Furthermore, low heat fluxes measured on the oceanic trench slope offshore of Nicaragua and Central Chile indicate that increased hydrothermal fluid circulation occurred as a result of fault creation and reactivation before subduction[8]. Also, the analysis of data from ocean-floor seismometers placed offshore of the Middle American and Southern Chilean trench revealed a continuous, swarm-like seismic activity distributed in the upper 15–20 km of the Cocos[5] and Nazca slabs[7], respectively, suggesting that fluids are present at mantle depths.

Slab serpentinization at mantle depths has important implications for numerous processes occurring in the upper mantle. In particular, it may (1) establish a more vigorous rheological weakening and partial melting of the mantle wedge, (2) enable the formation (at intermediate depths and in the cold core of the slab) of a dense, hydrous magnesium silicate phase, which is able to transport fluids down to lower mantle depths[12], and (3) produce a thick anisotropic layer in the upper part of the slab, which could significantly affect the pattern of anisotropy observed at subduction zones[13]. In addition, deep slab hydration has consequences for arc magma chemistry[5,19] and possibly for intra-slab seismicity at depth (see, for example, refs 20–22).

Aside from the above-mentioned implications, the results of the numerical experiments support our new concept of the spontaneous and deep hydration of the slab in the bending zone, in which downward fluid pumping inside the deforming medium is primarily controlled by the inverted subhydrostatic, or even negative, pressure gradients, localized along bending-related normal faults. Second, fluid flow can be locally modulated either by porosity enhancement due to prefailure dilatancy[9], pre-existing cracks[10] and migrating fluid-filled cracks[11], or by porosity reduction due to fault self-healing and serpentinization (see Supplementary Methods section). Additionally, the same concept can be applied

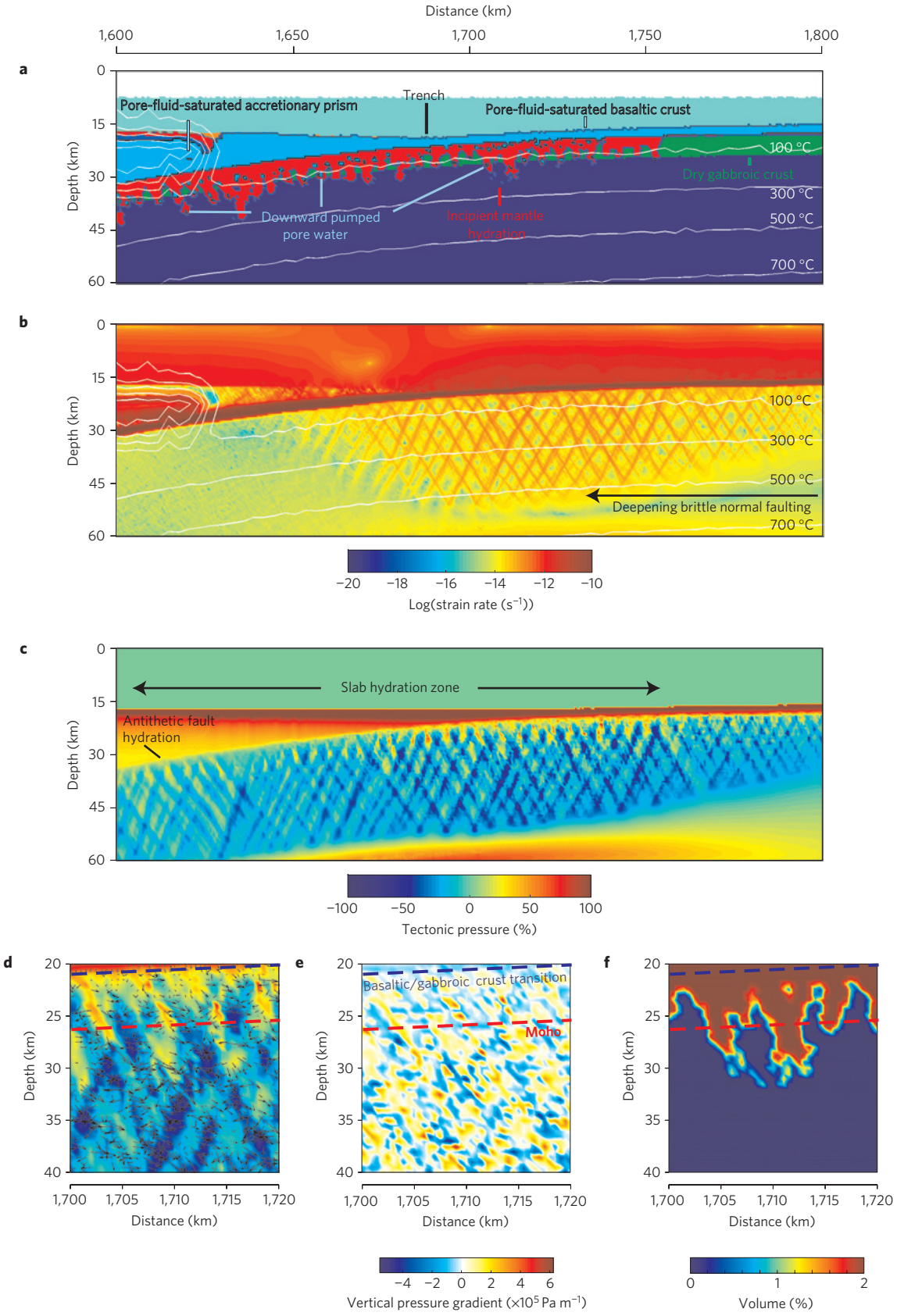

Figure 2 | Dynamics of deep slab hydration. a, Compositional map of the trench area. **b**, Strain-rate map. Fault activation due to the bending of the plate starts at shallow depths offshore of the trench and progressively deepens, **c**, Tectonic pressure map. **d**, Enlargement of the tectonic pressure map in proximity to the incipient mantle-hydration area (see Fig. 2a). The black arrows indicate inverted (that is, subhydrostatic) tectonic pressure gradients only. **e**, Vertical component of the tectonic pressure gradients with hydrostatic component subtracted (blue is subhydrostatic). **f**, Volumetric degree of hydrated rocks inside the slab whose maximum water content is set to 2 wt% (see Methods).

to strike-slip or extensional settings to explain fluid regimes dominated, down to depths of 15 km, by the infiltration of meteoric water, which when mixed with deeper source fluids produces vein mineralization[23–25].

Methods

The numerical experiments were carried out with the code I2ELVIS (ref. 26). The initial set-up is shown in Supplementary Fig. S1. The model uses variable grid spacing in both the horizontal and vertical directions. In the range from 100 km to the right of the trench to 300 km to the left of the trench, the horizontal grid resolution is 0.5 km. Elsewhere, the resolution increases gradually from 1 km up to 30 km. To continually resolve the subduction process, the horizontal grid resolution moves together with the retreating slab. Vertical resolution is 0.5 km for the first 100 km and then increases with depth to a maximum of 30 km. Subduction starts spontaneously as the result of the juxtaposition of two plates of different ages (1 Myr and 100 Myr for the left and right plates, respectively) along a transform fault that is assumed to be weak owing to water percolation and hydration of the boundary (low plastic strength of 1 MPa; refs 27, 28). In contrast to ref. 27, we also impose low plastic strength for the fluid-saturated subducting basaltic crust (see Supplementary Table S1) acting as a lubricating layer[28]. This ensures that a retreating, one-sided subduction of the negatively buoyant and older slab can initiate spontaneously without imposing any convergence, being driven solely by growing slab pull and, to a minor extent, by ridge push. The thermal structure of the initial plate set-up is computed according to the cooling of a semi-infinite, half-space equation[29]:

$$T = T_1 + (T_0 - T_1)\left(1 - erf\,(\eta)\right)$$

$$\eta = \frac{z}{2\sqrt{\kappa\,\tau}}$$

where $T_0 = 0\,^{\circ}\mathrm{C}$ for both plates, $T_1 = 1{,}270\,^{\circ}\mathrm{C}$ and $1{,}350\,^{\circ}\mathrm{C}$ for the young and old plates, respectively, κ is the thermal diffusivity (10^{-6} m^2 s^{-1}), τ is the age in seconds of the plates and η is the dimensionless similarity variable. The age of the older plate decreases linearly toward the right boundary, corresponding to a mid-ocean ridge (0 Myr). Although mantle rocks have the capacity to absorb up to 13 wt% water during serpentinization, we adopt 2 wt% water as an upper limit to account for the incomplete and heterogeneous hydration of the dry mafic and ultramafic rocks according to the implemented thermodynamic database[30]. Rheological parameters used in the model are listed in Supplementry Table S1. Brittle weakening is linearly dependent on plastic finite strain (ε) according to

$$\sin\gamma = \sin\gamma_0 + (\sin\gamma_1 - \sin\gamma_0)\frac{\varepsilon}{\varepsilon_1}$$

where $\sin\gamma$, $\sin\gamma_0$ and $\sin\gamma_1$ are the computed, the initial and the minimum value of the coefficient of friction, respectively. The minimum coefficient of friction ($\sin\gamma_1$) is established for plastic finite strains $\varepsilon \geq \varepsilon_1 = 1$ for all the lithologies. A high-viscosity lower boundary (10^{21} Pa s, from 680 to 700 km depth) is imposed to simulate the transition from the upper to the lower mantle.

Received 20 February 2009; accepted 11 September 2009; published online 11 October 2009

References

1. Masson, D. G. Fault patterns at outer trench walls. *Mar. Geophys. Res.* **13,** 209–225 (1991).
2. Ranero, C. R., Phipps Morgan, J. & Reichert, C. Bending-realted faulting and mantle serpentinization at the Middle America trench. *Nature* **425,** 367–373 (2003).
3. Ranero, C. R., Villaseñor, A., Phipps Morgan, J. & Weinrebe, W. Relationship between bend-faulting at trenches and intermediate-depth seismicity. *Geochem. Geophys. Geosys.* **6,** Q12002 (2005).
4. Ranero, C. R. & Sallares, V. Geophysical evidence for hydration of the crust and mantle of the Nazca plate during bending at the North Chile trench. *Geology* **32,** 549–554 (2004).
5. Grevemeyer, I., Ranero, C. R., Flueh, E. R., Kläschen, D. & Bialas, J. Passive and active seismological study of bending-related faulting and mantle serpentinization at the Middle America trench. *Earth Planet. Sci. Lett.* **258,** 528–542 (2007).
6. Contreras-Reyes, E., Grevemeyer, I., Flueh, E. R. & Reichert, C. Upper lithospheric structure of the subduction zone offshore of southern Arauco peninsula, Chile, at ~38° S. *J. Geophys. Res.* **113,** B07303 (2008).
7. Tilmann, F. J., Grevemeyer, I., Flueh, E. R., Dahm, T. & Gossler, J. Seismicity in the outer rise offshore southern Chile: Indication of fluid effects in crust and mantle. *Earth Planet. Sci. Lett.* **269,** 41–55 (2008).
8. Grevemeyer, I., Kaul, N., Diaz-Naveas, J. L., Villinger, H. W., Ranero, C. R. & Reichert, C. Heat flow and bending-related faulting at subduction trenches: Case studies offshore of Nicaragua and Central Chile. *Earth Planet. Sci. Lett.* **236,** 238–248 (2005).
9. Sibson, R. H. in *Geofluids: Origin, Migration and Evolution of Fluids in Sedimentary Basins* (ed. Parnell, J.) 69–84 (Geol. Soc. Spec. Publ. Vol. 78, 1994).
10. Korenaga, J. Thermal cracking and the deep hydration of oceanic lithosphere: A key to the generation of plate tectonics? *J. Geophys. Res.* **112,** B05408 (2007).
11. Phipps Morgan, J. & Holtzman, B. K. Vug-waves: A mechanism for coupled rock deformation and fluid migration. *Geochem. Geophys. Geosys.* **6,** Q08002 (2005).
12. Ohtani, E., Litasov, K., Hosoya, T., Kubo, T. & Kondo, T. Water transport into the deep mantle and formation of a hydrous transition zone. *Phys. Earth Planet. Inter.* **143–144,** 255–269 (2004).
13. Faccenda, M., Burlini, L., Gerya, T. V. & Mainprice, D. Fault-induced seismic anisotropy by hydration in subducting oceanic plates. *Nature* **455,** 1097–1100 (2008).
14. Johnson, H. P. & Pruis, M. J. Fluxes of fluid and heat from the oceanic crustal reservoir. *Earth Planet. Sci. Lett.* **216,** 565–574 (2003).
15. Mancktelow, N. Tectonic pressure: Theoretical concepts and modelled examples. *Lithos* **103,** 149–177 (2008).
16. Katz, R., Spiegelman, M. & Holtzman, B. The dynamics of melt and shear localization in partially molten aggregates. *Nature* **442,** 676–679 (2006).
17. Manning, C. E. & Ingebritsen, S. E. Permeability of the continental crust: Implications of geothermal data and metamorphic systems. *Rev. Geophys.* **37,** 127–150 (1999).
18. Mitchell, T. M. & Faulkner, D. R. Experimental measurements of permeability evolution during triaxal compression of initially intact crystalline rocks and implications for fluid flow in fault zone. *J. Geophys. Res.* **113,** B11412 (2008).
19. Rüpke, L. H., Morgan, J. P., Hort, M. & Connolly, J. A. D. Are the regional variations in Central American arc lavas due to differing basaltic versus peridotitic slab sources of fluids? *Geology* **30,** 1035–1038 (2002).
20. Brudzinski, M. R., Thurber, C. H., Hacker, B. R. & Engdahl, E. R. Global prevalence of double Benioff zones. *Science* **316,** 1472–1474 (2007).
21. Peacock, S. M. Are the lower planes of double seismic zones caused by serpentine dehydration in subducting oceanic mantle? *Geology* **29,** 299–302 (2001).
22. Yamasaki, T. & Seno, T. Double seismic zone and dehydration embrittlement of the subducting slab. *J. Geophys. Res.* **108,** 2212 (2003).
23. Nesbitt, B. E. & Muehlenbachs, K. Origins and movement of fluids during deformation and metamorphism in the Canadian Cordillera. *Science* **245,** 733–736 (1989).
24. McLellan, J. G., Oliver, N. H. S. & Schaubs, P. M. Fluid flow in extensional environments; numerical modelling with an application to Hamersley iron ores. *J. Struct. Geol.* **26,** 1157–1171 (2004).
25. Sheldon, H. A. & Ord, A. Evolution of porosity, permeability and fluid pressure in dilatant faults post-failure: Implications for fluid flow and mineralization. *Geofluids* **5,** 272–288 (2005).
26. Gerya, T. V. & Yuen, D. A. Robust characteristic method for modeling multiphase visco-elasto-plastic thermo-mechanical problems. *Phys. Earth Planet. Inter.* **163,** 83–105 (2007).
27. Hall, C. E., Gurnis, M., Sdrolias, M., Lavier, L. L. & Muller, R. D. Catastrophic initiation of subduction following forced convergence across fractures zones. *Earth Planet. Sci. Lett.* **212,** 15–30 (2003).
28. Gerya, T. V., Connolly, J. A. D. & Yuen, D. A. Why is terrestrial subduction one-sided? *Geology* **36,** 43–46 (2008).
29. Turcotte, D. L. & Schubert, G. *Geodynamics* (Cambridge Univ. Press, 2002).
30. Gerya, T. V., Connolly, J. A. D., Yuen, D. A., Gorczyk, W. & Capel, A. M. Seismic implications of mantle wedge plumes. *Phys. Earth Planet. Inter.* **156,** 59–74 (2006).

Acknowledgements

This work was supported by SNF Research Grants 200021-113672/1, 200021-113672/1 and 200021-116381/1, ETH Research Grants TH-12/05-3 and TH-0807-3 and ETH account 0-12422-97. M.F. thanks N. Mancktelow for discussion about tectonic pressure effects on fluid flow in subducting slabs. M. Spiegelman contributed to clarify the basic concepts of this work. D. May improved the English of the manuscript.

Author contributions

M.F. designed the study, carried out and analysed the numerical experiments and wrote the paper. T.V.G. developed the numerical code and analysed the numerical experiments. L.B. contributed to the concept development. All authors discussed the results and commented on the paper.

Additional information

Supplementary information accompanies this paper on www.nature.com/naturegeoscience. Reprints and permissions information is available online at http://npg.nature.com/reprintsandpermissions. Correspondence and requests for materials should be addressed to M.F.